The effects of the Dzyaloshinskii–Moriya interaction on the ground-state properties of the *XY* chain in a transverse field*

Zhong Ming(钟 鸣)[a], Xu Hui(徐 卉)[a], Liu Xiao-Xian(刘小贤)[a], and Tong Pei-Qing(童培庆)[a,b,†]

[a] *Department of Physics and Institute of Theoretical Physics, Nanjing Normal University, Nanjing* 210023, *China*

[b] *Jiangsu Key Laboratory for Numerical Simulation of Large Scale Complex Systems, Nanjing Normal University, Nanjing* 210023, *China*

(Received 19 December 2012; revised manuscript received 27 March 2013)

The effects of the Dzyaloshinski–Moriya (DM) interaction on the ground-state properties of the anisotropic *XY* chain in a transverse field have been studied by means of correlation functions and entanglement. Different from the case without the DM interaction, the excitation spectra ε_k of this model are not symmetrical in the momentum space and are not always positive. As a result, besides the ferromagnetic (FM) and the paramagnetic (PM) phases, a gapless chiral phase is induced. In the chiral phase, the von Neumann entropy is proportional to $\log_2 L$ (L is the length of a subchain) with the coefficient $A \approx 1/3$, which is the same as that of the *XY* chain in a transverse field without the DM interaction for $\gamma = 0$ and $0 < h \leq 1$. And in the vicinity of the critical point between the chiral phase and the FM (or PM) phase, the behaviors of the nearest-neighbor concurrence and its derivative are like those for the anisotropy transition.

Keywords: Dzyaloshinskii–Moriya interaction, the *XY* chain in a transverse field, quantum entanglement, ground-state properties

PACS: 03.67.Mn, 75.10.Jm, 73.43.Nq, 75.40.Cx **DOI:** 10.1088/1674-1056/22/9/090313

1. Introduction

In recent years, the antisymmetric Dzyaloshinskii–Moriya (DM) interaction has received much attention. The DM interaction introduced by Dzyaloshinskii[1] and Moriya[2] is a combination of super-exchange and spin–orbital interactions, which can provide the microscopic mechanism for the coexistence of ferroelectricity and incommensurate magnetism in many multiferroics.[3–5] Some quantum antiferromagnetic systems are described by the DM interaction with underlying helical magnetic structures, such as Cu benzoate,[6,7] Yb_4As_3,[8] Cs_2CuCl_4,[9] $BaCu_2Si_2O_7$,[10] and kagome antiferromagnets.[11,12] Other materials, such as an Fe double layer and a wheel single-molecule magnet, have also been studied with the DM interaction.[13,14]

Besides those real materials, one-dimensional spin chains with the DM interaction have also been studied extensively.[15–23] For example, the phase diagram of the Ising model (without external field) with the DM interaction was studied with the quantum renormalization-group (QRG) method, in which a quantum critical point separates the antiferromagnetic phase and the chiral phase.[15] The phase diagram of the *XXZ* model with the DM interaction was also obtained with the QRG approach; three phases (ferromagnetic, spin-fluid, and Neel phases) were found.[16] The dynamic properties of the *XXZ* and the *XY* chains with the DM interaction have also been studied.[17,18] Very recently, the effects of the DM interaction on the quantum and classical correlations[24] of the one-dimensional *XY* chain in a transverse field were studied. Unfortunately, the authors used incorrect excitation spectra, which brought doubts to their results. In fact, the excitation spectra and the critical points of the anisotropic *XY* chain with the DM interaction were firstly found by Siskens *et al.*,[25] however the properties of the excitation spectra did not arouse enough attention. It should be noticed that the excitation spectra ε_k of this model are not symmetrical in the momentum space and are not always greater than zero, which may cause some special behaviors of the system.

On the other hand, quantum entanglement is viewed as a main ingredient in quantum information processes and has attracted considerable interest in various fields of physics. In the last decade, much attention has been paid to the relationship between quantum entanglement and quantum phase transitions (QPTs) (see Ref. [26] for a review). There are two widely used measures of entanglement for spin systems. One is the concurrence,[27] and the other is the von Neumann entropy.[28] By using the concurrence, Osterloh *et al.*[29] found that for the anisotropic *XY* chain in a transverse field, the derivative of the nearest-neighbor concurrence presents a logarithmic divergence for an infinite system in the vicinity of the critical point $h = 1$, which is related to the critical properties of the Ising transition.[30] For the same model, we found that[31] the derivative of the nearest-neighbor concurrence changes little with the increasing system size N in the vicinity of the critical point $\gamma = 0$ ($0 < h \leq 1$) corresponding to the anisotropy transi-

*Project supported by the National Natural Science Foundation of China (Grant Nos. 11205090 and 11175087) and the Natural Science Foundation of the Jiangsu Higher Education Institutions of China (Grant No. 12KJB140008).

†Corresponding author. E-mail: pqtong@njnu.edu.cn

© 2013 Chinese Physical Society and IOP Publishing Ltd

tion. And Vidal *et al.* found that[32] the von Neumann entropy S_L is a constant in the noncritical region and $S_L \sim (c\log_2 L)/3$ at the critical points. The coefficient is given by the central charge c in the conformal field theory,[33] $c = 1/2$ at $h = 1$ while $c = 1$ at $\gamma = 0$ ($0 < h \leq 1$). However, for the anisotropic XY chain in a transverse field with the DM interaction, the formulas used to calculate the concurrence and the von Neumann entropy should be both improved, which results from the characteristics of the excitation spectra. We will study the effects of the DM interaction on the entanglement of this model in detail.

The paper is organized as following. In Section 2, the model is given. In Section 3, we obtain the detailed phase diagram by analytical and numerical methods. In Section 4, we discuss the behaviors of entanglement. A brief conclusion is given in Section 5.

2. Model

The Hamiltonian of the XY chain with the DM interaction (in the z direction) in a transverse field reads[17]

$$H = -\sum_{n=1}^{N}\left(\frac{1+\gamma}{2}\sigma_n^x\sigma_{n+1}^x + \frac{1-\gamma}{2}\sigma_n^y\sigma_{n+1}^y + h\sigma_n^z\right) - \sum_{n=1}^{N} D(\sigma_n^x\sigma_{n+1}^y - \sigma_n^y\sigma_{n+1}^x), \quad (1)$$

where N is the number of spins in the chain, γ ($-1 \leq \gamma \leq 1$) is the anisotropy parameter of the system, D is the strength of the DM interaction, $\sigma^{x,y,z}$ are the Pauli matrices, and h is a uniform external transverse field.

By using the Jordan–Wigner transformation,[34] Hamiltonian (1) can be written with spinless fermion operators $c_n^\dagger$ and c_n, which yields

$$H = -\sum_{n=1}^{N}\{[(1+2\mathrm{i}D)c_n^\dagger c_{n+1} + \gamma c_n^\dagger c_{n+1}^\dagger + hc_n^\dagger c_n] + \text{h.c.}\} + \sum_{n=1}^{N} h. \quad (2)$$

Through Fourier transforms of the fermionic operators, $c_n = \sum_k c_k \mathrm{e}^{-\mathrm{i}kn}/\sqrt{N}$ (here $k = 2p\pi/N$ for odd N and periodic boundary condition or for even N and antiperiodic boundary condition, $p = -(N-1)/2, -(N-3)/2, \ldots, (N-3)/2, (N-1)/2$), Hamiltonian (2) can be written in the momentum space and be reduced to the diagonal form

$$H = \sum_{k=-\pi}^{\pi} \varepsilon_k(\eta_k^\dagger\eta_k - 1/2) \quad (3)$$

with[25]

$$\varepsilon_k = -4D\sin k + 2\sqrt{(\cos k + h)^2 + \gamma^2\sin^2 k} \quad (4)$$

by the Bogoliubov transformation

$$c_k = u_k\eta_k + v_{-k}^*\eta_{-k}^\dagger. \quad (5)$$

$$u_k = \frac{\alpha_k - \sqrt{\beta_k}}{\sqrt{2(\beta_k - \alpha_k\sqrt{\beta_k})}} = \cos\theta_k,$$

$$v_k = \frac{\mathrm{i}\gamma\sin k}{\sqrt{2(\beta_k - \alpha_k\sqrt{\beta_k})}} = \mathrm{i}\sin\theta_k, \quad (6)$$

with $\alpha_k = \cos k + h$ and $\beta_k = \alpha_k^2 + \gamma^2\sin^2 k$.

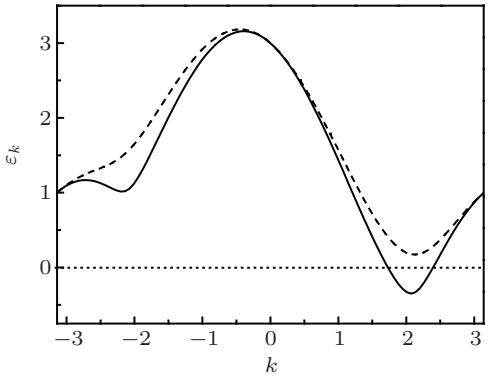


Fig. 1. Two typical excitation spectra. The solid and dashed lines correspond to $D = 0.2$, $\gamma = 0.2$, $h = 0.5$ and $D = 0.2$, $\gamma = 0.5$, $h = 0.5$, respectively. The dotted line corresponds to $\varepsilon_k = 0$.

The forms of u_k and v_k are independent of D and the same as those in the XY model without the DM interaction. But the excitation spectra ε_k are not symmetrical in the momentum space and not always greater than zero. Figure 1 shows two typical examples, in which ε_k are positive for all k when $D = 0.2$, $\gamma = 0.5$, $h = 0.5$, while they are negative for $1.7 < k < 2.4$ when $D = 0.2$, $\gamma = 0.2$, $h = 0.5$. In the thermodynamic limit ($N \to \infty$), the ground state $|G\rangle$ of the system corresponds to the configuration in which all states with $\varepsilon_k < 0$ are filled and those with $\varepsilon_k \geq 0$ are empty, that is

$$\begin{cases} \eta_k|G\rangle = 0, & (\varepsilon_k \geq 0), \\ \eta_k^\dagger|G\rangle = 0, & (\varepsilon_k < 0). \end{cases} \quad (7)$$

The $|G\rangle$ can be written as $|G\rangle = \prod_{k>0} G_k$, and G_k can be derived from the transformation $\eta_k = u_k c_k + v_{-k}c_{-k}^\dagger$

$$\begin{cases} G_k = \cos\theta_k|0\rangle_k|0\rangle_{-k} + \mathrm{i}\sin\theta_k|1\rangle_k|1\rangle_{-k}, & (\varepsilon_k \geq 0), \\ G_k = |1\rangle_k|0\rangle_{-k}, & (\varepsilon_k < 0), \end{cases} \quad (8)$$

with $|0\rangle_k$ and $|1\rangle_k$ corresponding to the vacuum and the occupied states of c_k, respectively.

It must be pointed out that the above ground state is very different from that used in Ref. [24] coming from incorrect excitation spectra, where ε_k are always larger than or equal to zero. Furthermore, because ε_k may be negative, the formulas used to calculate the correlation functions, the concurrence, and the von Neumann entropy should be modified, which will be discussed in detail in the following.

3. Phase diagram

In view of the symmetry of Hamiltonian (1), here we consider the case of γ, D, $h \geq 0$. We use the general Lee–Yang method[35] to find critical points. According to this method, we solve equation $\varepsilon_k(h) = 0$ in a complex h plane. The solutions at the positive real axis correspond to the QPT points.

From excitation spectra (4), the solution of $\varepsilon_k(h) = 0$ in a complex h plane is

$$h = -\cos k + \sqrt{4D^2 - \gamma^2}\sin k. \tag{9}$$

Three cases can be discussed.

(i) $D = 0$, which corresponds to the XY chain in a transverse field. Equation (9) can be transformed to $h = -\cos k + \mathrm{i}\gamma\sin k$. There are two distinct critical lines, the line $h = 1$ and the line segment $h \in (0, 1)$ with $\gamma = 0$. The phase diagram is shown in Fig. 3(a). As it is well known, region I corresponds to a ferromagnetic (FM) phase ordered along the x direction (FM_x), while region II corresponds to a disordered paramagnetic (PM) phase. Following the standard notation, we refer to the QPT across the critical line $h = 1$ driven by the transverse magnetic field as the Ising transition, and the QPT across the critical line $\gamma = 0$ driven by the anisotropy parameter γ as the anisotropy transition.

(ii) $0 < D < 0.5$. If $\gamma > 2D$, Eq. (9) can be transformed to $h = -\cos k + \mathrm{i}\sqrt{\gamma^2 - 4D^2}\sin k$. It is easy to check that the solutions, which lie on an ellipse, are cutting the positive real axis at $h = 1$ in the complex h plane (see Fig. 2(a)). If $\gamma \leq 2D$, Eq. (9) can be written as $h = -\cos k + \sqrt{4D^2 - \gamma^2}\sin k$. The solutions are always real and the maximal value is $h = \sqrt{4D^2 - \gamma^2 + 1}$, so they are all critical points from $h = 0$ to $h = \sqrt{4D^2 - \gamma^2 + 1}$ (see Fig. 2(b)). The phase diagram is shown in Fig. 3(b), which is composed of three regions. Regions I and II are noncritical regions with an energy gap, while region III is a critical region without an energy gap. The vertical solid line corresponds to $h = 1$, the horizontal solid line corresponds to $\gamma = 2D$, and the curved solid line corresponds to $h = \sqrt{4D^2 - \gamma^2 + 1}$.

(iii) $D \geq 0.5$. The γ is always smaller than $2D$ for $\gamma \leq 1$, so the points from $h = 0$ to $h = \sqrt{4D^2 - \gamma^2 + 1}$ are all critical points . The phase diagram is showed in Fig. 3(c). The curved solid line also corresponds to $h = \sqrt{4D^2 - \gamma^2 + 1}$.

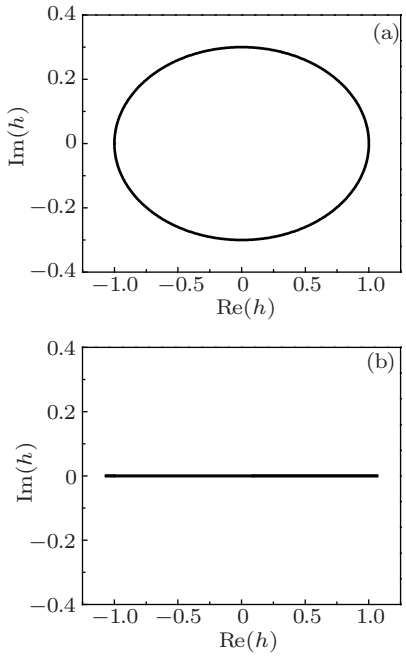


Fig. 2. The solution of $\varepsilon_k(h) = 0$ in the complex h plane with (a) $\gamma = 0.5$ or (b) $\gamma = 0.05$. Here $D = 0.2$.

In the above three cases, $\varepsilon_k > 0$ for all k in regions I and II, while $\varepsilon_k < 0$ for more than one k in region III. Obviously, region III may correspond to a special phase. Because the phase diagram shown in Fig. 3(b) contains most of the phases, as long as we make clear the properties of this phase diagram, the properties of the other will also be understood. Therefore, in this paper, we focus on the study of the QPTs in the case of $0 < D < 0.5$. In the following calculations, we take $D = 0.2$ without loss of generality.

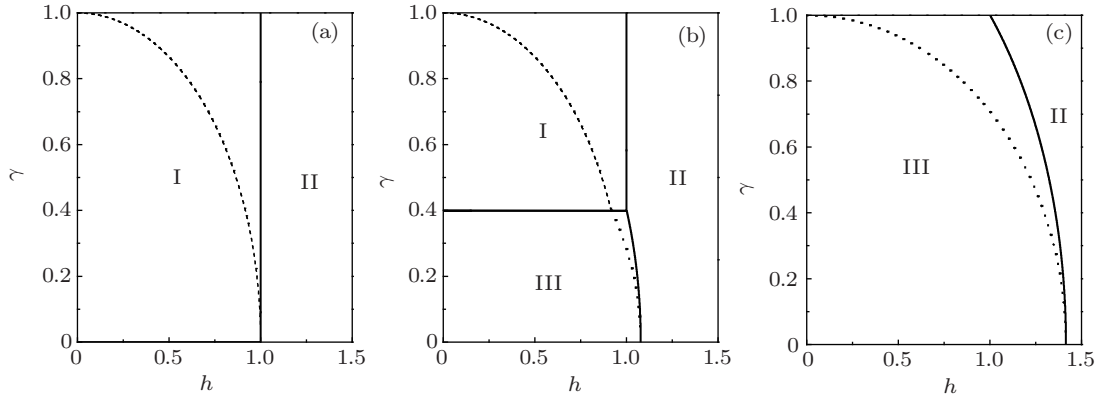


Fig. 3. The phase diagrams for (a) $D = 0$, (b) $D = 0.2$, and (c) $D = 0.5$. Regions I, II, and III between the solid lines and coordinate axes correspond to FM, PM, and chiral phases, respectively. The dashed lines in region I of panels (a) and (b) correspond to $h = \sqrt{1 - \gamma^2}$, while the dotted lines in region III of panels (b) and (c) correspond to $h = \sqrt{4D^2 - 2\gamma^2 + 1}$, which are discussed in Section 4.

In order to study the properties of each phase of this model, we study correlation function $C_L^x = C_{1,N/2}^x = \langle \sigma_1^x \sigma_{N/2}^x \rangle$ and the chiral order parameter in the z direction[36]

$$C_h = \frac{1}{4N} \sum_{i=1}^{N} \langle \sigma_i^x \sigma_{i+1}^y - \sigma_i^y \sigma_{i+1}^x \rangle. \tag{10}$$

Usually, the phase with $C_L^x \neq 0$ is referred to as the FM phase ordered along the x direction, while the phase with $C_L^x = 0$ is referred to as the PM phase. And the phase with $C_h \neq 0$ is referred to as the chiral phase.

For this model, the chiral order parameter is

$$C_h = \frac{1}{N} \sum_k \Theta(\varepsilon_k) \sin k, \tag{11}$$

where

$$\Theta(x) = \begin{cases} 1, & x \geq 0, \\ 0, & x < 0. \end{cases}$$

Obviously, $C_h = 0$ in regions I and II where ε_k are always positive.

However, the correlation function C_L^x should be discussed in detail. From the Jordan–Wigner transformation,[34] we have

$$C_{1,n}^x = \langle \sigma_1^x \sigma_n^x \rangle = \langle B_1 A_2 B_2 A_3 \ldots B_{n-1} A_n \rangle, \tag{12}$$

with $A_n = c_n^\dagger + c_n$ and $B_n = c_n^\dagger - c_n$. This can be calculated by using the Wick theorem in terms of the products of the expectation values of just two operators. The basic contractions are

$$\begin{aligned} G_{ln} &= \langle B_l A_n \rangle = -\langle A_n B_l \rangle \\ &= \frac{1}{N} \sum_k \mathrm{sgn}(-\varepsilon_k) \cos[(n-l)k - 2\theta_k], \end{aligned} \tag{13}$$

$$\begin{aligned} \langle A_l A_n \rangle &= -\langle B_l B_n \rangle \\ &= \begin{cases} -\frac{2\mathrm{i}}{N} \sum_k \Theta(\varepsilon_k) \sin(n-l)k, & n \neq l, \\ 1, & n = l, \end{cases} \end{aligned} \tag{14}$$

where θ_k are defined in Eq. (6).

In regions I and II,

$$\langle A_l A_n \rangle = -\langle B_l B_n \rangle = \delta_{ln}, \tag{15}$$

as ε_k are greater than zero for all k. Because $\langle A_l A_l \rangle$ and $\langle B_l B_l \rangle$ never occur,

$$C_{1,n}^x = \begin{vmatrix} G_{1,2} & G_{1,3} & \ldots & G_{1,n} \\ \vdots & \vdots & \vdots & \vdots \\ G_{n-1,2} & G_{n-1,3} & \ldots & G_{n-1,n} \end{vmatrix}. \tag{16}$$

In region III, ε_k may be negative for some k , thus $\langle A_l A_n \rangle$ and $\langle B_l B_n \rangle$ are nonzero even if $n \neq l$. Therefore,[37]

$$C_{1,n}^x = (U)^{1/2}, \tag{17}$$

where

$$U = \begin{vmatrix} 0 & \langle B_1 A_2 \rangle & \langle B_1 B_2 \rangle & \langle B_1 A_3 \rangle & \ldots & \langle B_1 A_n \rangle \\ -\langle B_1 A_2 \rangle & 0 & \langle A_2 B_2 \rangle & \langle A_2 A_3 \rangle & \ldots & \langle A_2 A_n \rangle \\ -\langle B_1 B_2 \rangle & -\langle A_2 B_2 \rangle & 0 & \langle B_2 A_3 \rangle & \ldots & \langle B_2 A_n \rangle \\ \ldots & \ldots & \ldots & 0 & \ldots & \ldots \\ -\langle B_1 A_n \rangle & -\langle A_2 A_n \rangle & \ldots & \ldots & \ldots & 0 \end{vmatrix}. \tag{18}$$

Figure 4 gives C_L^x as a function of h for different γ. We can find that from region I to region II with $\gamma > 2D$ (the solid line), C_L^x continuously decreases to zero at $h = 1$, and from region III to region II with $\gamma < 2D$ (the dashed line), C_L^x is always zero.

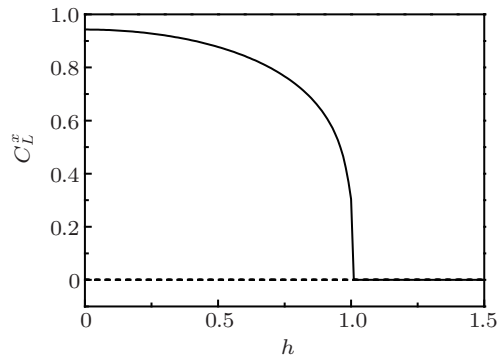


Fig. 4. Correlation function C_L^x as a function of h. The solid and dashed lines correspond to $\gamma = 0.5$ and 0.2, respectively. Here $D = 0.2$.

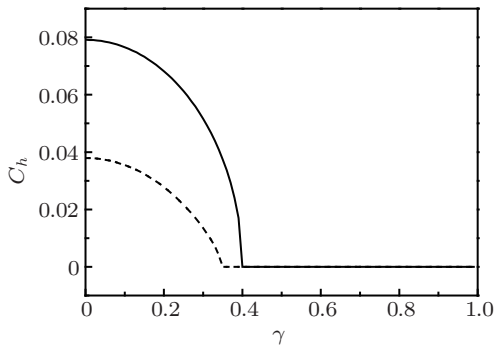


Fig. 5. Chiral order parameter C_h as a function of γ. The solid and dashed lines correspond to $h = 0.8$ and 1.02, respectively. Here $D = 0.2$.

Figure 5 gives C_h as a function of γ for different h. We can find that from region III to region I with $h < 1$ (the solid line), C_h continuously decreases to zero at $\gamma = 2D$. From region III to region II with $1 < h < \sqrt{1+4D^2}$ (the dashed line), C_h continuously decreases to zero at $\gamma = \sqrt{4D^2 - h^2 + 1}$. The non-analytic points of C_L^x and C_h do agree with the critical points

found by the Lee–Yang method (see Fig. 3(b)).

According to the above numerical results, we can find that in region I, $C_L^x \neq 0$ and $C_h = 0$, which corresponds to the FM phase along the x axis. When $h \to 0$, there are two degenerate ferromagnetic ground states with all spins pointing either parallel or antiparallel to the x axis, $|\rightarrow\rightarrow\rightarrow\cdots\rightarrow\rangle$ or $|\leftarrow\leftarrow\leftarrow\cdots\leftarrow\rangle$. In region II, $C_L^x = 0$ and $C_h = 0$, which corresponds to the PM phase. When $h \gg 1$, the ground state is a paramagnet $|\uparrow\uparrow\uparrow\cdots\uparrow\rangle$ with all spins polarized up along the z axis. While in region III, $C_L^x = 0$ and $C_h \neq 0$, which corresponds to the chiral phase induced by the DM interaction. A classical picture[15] for this phase is that the spins orientate in the xy plane and the angle between neighboring spins has a nonzero value. It is worth mention that different from the FM and the PM phases, the chiral phase is gapless.

4. Quantum entanglement

In order to acquire a better understanding of the effects of the DM interaction on the ground-state entanglement, we study the concurrence and the Von Neumann entropy in this section.

4.1. Concurrence

Concurrence measures the entanglement between two spins and is calculated with the density matrix ρ_{ij} obtained from the ground-state wave function in which all the spins except those at positions i and j have been traced out. The concurrence between sites i and j is defined as

$$C_{ij} = \max\{0, r_1 - r_2 - r_3 - r_4\}, \tag{19}$$

where r_n are the square roots of the eigenvalues of the operator

$$R = \rho_{ij}(\sigma^y \otimes \sigma^y)\rho_{ij}^*(\sigma^y \otimes \sigma^y) \tag{20}$$

in decreasing order. Due to the symmetry of the Hamiltonian, the density matrix ρ_{ij} has the form

$$\rho_{ij} = \begin{pmatrix} a_{11} & 0 & 0 & a_{14} \\ 0 & a_{22} & a_{23} & 0 \\ 0 & a_{23}^* & a_{33} & 0 \\ a_{14}^* & 0 & 0 & a_{44} \end{pmatrix}. \tag{21}$$

The matrix elements can be expressed in terms of the various correlation functions

$$\begin{aligned} a_{11} &= \frac{1}{4}(1 + 2\langle\sigma_i^z\rangle + \langle\sigma_i^z\sigma_j^z\rangle), \\ a_{22} = a_{33} &= \frac{1}{4}(1 - \langle\sigma_i^z\sigma_j^z\rangle), \\ a_{44} &= \frac{1}{4}(1 - 2\langle\sigma_i^z\rangle + \langle\sigma_i^z\sigma_j^z\rangle), \\ a_{14} &= \frac{1}{4}[\langle\sigma_i^x\sigma_j^x\rangle - \langle\sigma_i^y\sigma_j^y\rangle - \mathrm{i}(\langle\sigma_i^x\sigma_j^y\rangle + \langle\sigma_i^y\sigma_j^x\rangle)], \\ a_{23} &= \frac{1}{4}[\langle\sigma_i^x\sigma_j^x\rangle + \langle\sigma_i^y\sigma_j^y\rangle + \mathrm{i}(\langle\sigma_i^x\sigma_j^y\rangle - \langle\sigma_i^y\sigma_j^x\rangle)]. \end{aligned} \tag{22}$$

It should be noticed that for the XY chain in a transverse field without the DM interaction, the Hamiltonian is real, $\rho_{ij} = \rho_{ij}^*$, therefore the imaginary parts of a_{14} and a_{23} are zero. While for the XY chain in a transverse field with the DM interaction, Hamiltonian (1) is complex, the imaginary parts of a_{14} and a_{23} are no longer zero.

Now we turn to discuss the behaviors of concurrence across those three critical lines in Fig. 3(b). In this paper, the nearest-neighbor concurrence C_{12} of sites 1 and 2 is considered.

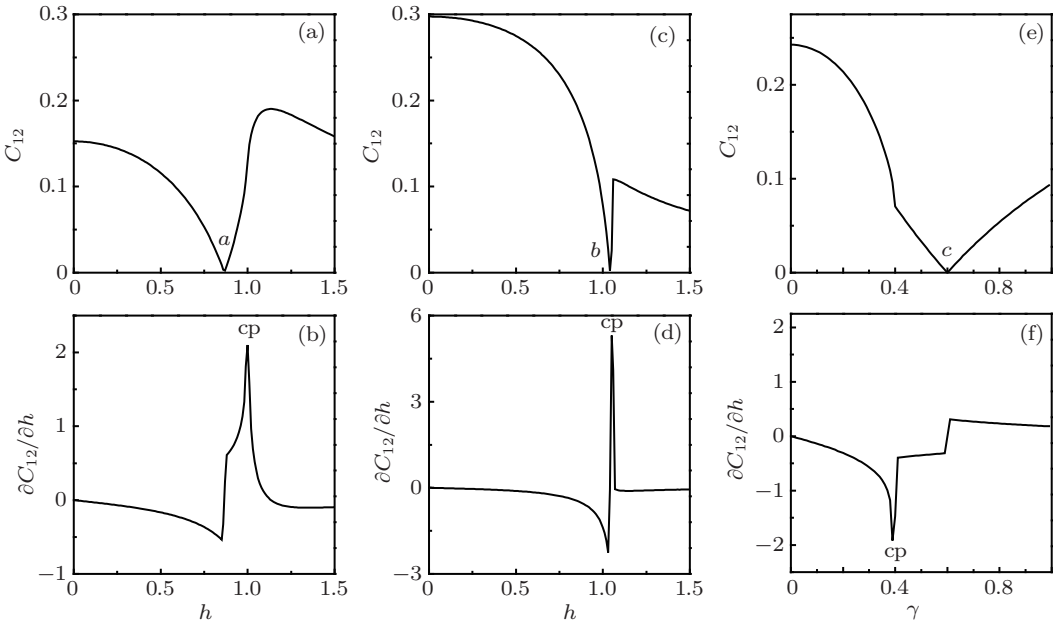


Fig. 6. The C_{12} as a function of h for (a) $\gamma = 0.5$ and (c) $\gamma = 0.2$. (e) The C_{12} as a function of γ for $h = 0.8$. Panels (b), (d), and (f) are the derivatives of the curves in panels (a), (c), and (e), respectively. Here $D = 0.2$, cp represents the critical point.

Figure 6 gives C_{12} and its derivative. Because the forms of u_k and v_k in Eq. (6) are independent of D and $\varepsilon_k > 0$ for all k in regions I and II, all the results of the correlation functions in Eq. (22) are the same as those of the XY model without the DM interaction. Therefore, the behaviors of C_{12} and its derivative in the vicinity of the critical point from region I to region II (see Figs. 6(a) and 6(b) for $\gamma = 0.5$) are related to the critical properties of the Ising transition.[29] However for the cases from region III to region II (see Figs. 6(c) and 6(d) for $\gamma = 0.5$) and from region III to region I (see Figs. 6(e) and 6(f) for $h = 0.8$), the derivative of C_{12} hardly changes with increasing N in the vicinity of the critical point and these behaviors are like the critical properties of the anisotropy transition.[31]

In addition, there are some other nonanalytic points, such as points a, b, and c in Fig. 6 corresponding to $C_{12} = 0$. For the XY chain in a transverse field without the DM interaction, $C_{12} = 0$ occurs at $h = \sqrt{1-\gamma^2}$,[38] which was first found by Barouch and McCoy.[39,40] Furthermore, Müller *et al.* found that at this boundary the ground state can be expressed as a product state.[41] The ground state is in fact doubly degenerated. This boundary is shown as a dashed line in Fig. 3(a). And the DM interaction may also affect this boundary. For $\gamma > 2D$, it still satisfies $h = \sqrt{1-\gamma^2}$, which is shown as a dashed line in Fig. 3(b). But for $0 < \gamma < 2D$, we find by numerical fitting that $C_{12} = 0$ at $h \approx \sqrt{4D^2 - 2\gamma^2 + 1}$, which is shown as dotted lines in Figs. 3(b) and 3(c).

4.2. Von Neumann entropy

Von Neumann entropy measures the entanglement between a block of L contiguous spins and the rest of the chain, which is defined as[42]

$$S_L = -\mathrm{Tr}(\rho_L \log_2 \rho_L). \tag{23}$$

Here, ρ_L is the reduced density matrix obtained from the ground-state wave function in which all the spins except first L contiguous spins have been traced out.

Following the standard procedure,[42] firstly, we consider two Majorana operators m_{2l} and m_{2l+1} for each site l of the N-spin chain, which are defined as

$$m_{2l+1} = \left(\prod_{j=0}^{l-1} \sigma_j^z\right)\sigma_l^x, \quad m_{2l} = \left(\prod_{j=0}^{l-1} \sigma_j^z\right)\sigma_l^y. \tag{24}$$

The operators m_n are Hermitian and obey the anticommutation relation $\{m_j, m_l\} = 2\delta_{jl}$. In the ground state, the correlation matrix with the expectation values $\langle m_j m_l \rangle$ is a $2N \times 2N$ matrix written as

$$\boldsymbol{\Gamma}_N = \begin{pmatrix} T_{11} & T_{12} & \dots & T_{1N} \\ \vdots & \vdots & \vdots & \vdots \\ T_{N1} & T_{N2} & \dots & T_{NN} \end{pmatrix}, \tag{25}$$

$$T_{jl} = \begin{pmatrix} g_{jl} & \mathrm{i}G_{jl} \\ -\mathrm{i}G_{lj} & g_{jl} \end{pmatrix}.$$

Here, G_{jl} are also defined by Eq. (13) and

$$g_{jl} = \frac{1}{N}\sum_{k=-\pi}^{\pi} \mathrm{e}^{-\mathrm{sgn}(\varepsilon_k)\mathrm{i}k(j-l)}.$$

We should note that when $D = 0$, $g_{jl} = \delta_{jl}$ and $\varepsilon_k \geq 0$ for all k. When $D \neq 0$, ε_k may be negative in some regions, so g_{jl} are no longer equal to δ_{jl}

$$g_{jl} = \begin{cases} 1, & \text{if } j = l, \\ \sum\limits_{k=-\pi}^{\pi} -\mathrm{i}\,\mathrm{sgn}(\varepsilon_k)\sin[k(j-l)], & \text{if } j \neq l. \end{cases}$$

However, we find that when $j \neq l$, g_{jl} are pure imaginary numbers and $g_{jl} = -g_{lj}$, so the $\boldsymbol{\Gamma}_N$ matrix is an antisymmetric matrix.

Secondly, considering L spins at sites 1,2, …, L, we can get a $2L \times 2L$ submatrix $\boldsymbol{\Gamma}_L$ from $\boldsymbol{\Gamma}_N$ by eliminating the rows and columns corresponding to those spins belong to the rest of the chain. Obviously, $\boldsymbol{\Gamma}_L$ is also antisymmetrical and can be always brought into a block-diagonal form

$$\overline{\boldsymbol{\Gamma}}_L = \boldsymbol{Q}\boldsymbol{\Gamma}\boldsymbol{Q}^{\mathrm{T}} = \boldsymbol{I} + \oplus_{n=0}^{L-1}\mathrm{i}v_n \begin{pmatrix} 0 & 1 \\ -1 & 0 \end{pmatrix}, \quad v_n \geq 0. \tag{26}$$

Here, $\boldsymbol{Q}$ is an orthogonal matrix, and $\boldsymbol{I}$ is a unit matrix. Therefore, the von Neumann entropy is given by[42]

$$S_L = \sum_{j=0}^{L-1}\left[-\frac{1+v_j}{2}\log_2\left(\frac{1+v_j}{2}\right) - \frac{1-v_j}{2}\log_2\left(\frac{1-v_j}{2}\right)\right]. \tag{27}$$

We find that the behaviors of the von Neumann entropy are similar in the same phase, so without loss of generality we only give S_L at some typical points in Fig. 7. In regions I (the solid line in Fig. 7(a)) and II (the dashed line in Fig. 7(a)), S_L is a non-zero constant when the block is large enough. Differently, in region III, S_L is proportional to $\log_2 L$ with the coefficient $A \approx 1/3$ (the dashed and dotted lines in Fig. 7(b)), which is the same as that of the XY chain in a transverse field without the DM interaction for $\gamma = 0$ and $0 < h \leq 1$, so the whole region represents the critical property. In the critical line $h = 1$, S_L is proportional to $\log_2 L$ with the coefficient $A \approx 1/6$ (the solid line in Fig. 7(b)), which is the same as that in the Ising transition line of the XY chain in a transverse field without the DM interaction.

Especially, on the dashed line of Fig. 3(b), where the relationship between h and γ satisfies $h = \sqrt{1-\gamma^2}$ for $\gamma > 2D$, there is $S_L = 1$ and the ground state is doubly degenerated. For example, the result of S_L at the point $(h, \gamma) = (0.866, 0.5)$ is shown as a dotted line in Fig. 7(a). However, for $0 < \gamma < 2D$, $S_L \sim (\log_2 L)/3$, even if $h = \sqrt{4D^2 - 2\gamma^2 + 1}$ (the dotted line in Fig. 7(b)) while $C_{12} = 0$.

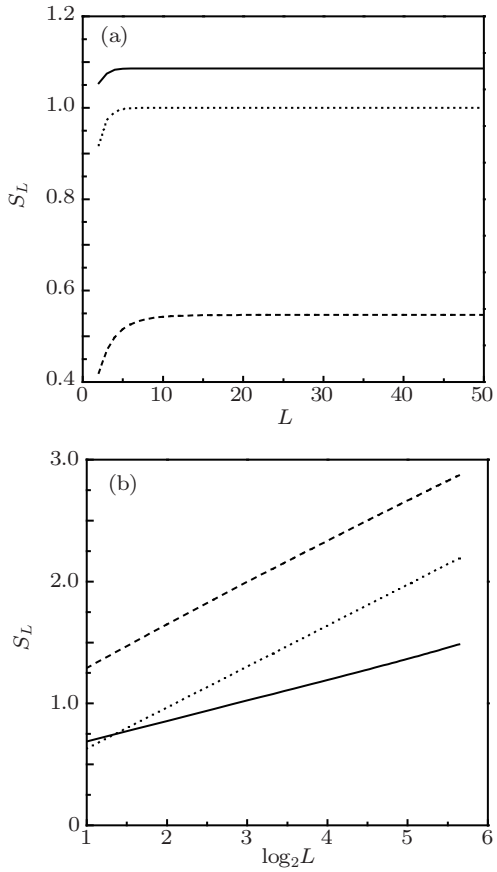


Fig. 7. (a) The S_L as a function of L in noncritical regions. The solid, dashed, and dotted lines correspond to the points $h = 0.5$, 1.1, 0.866 with $D = 0.2$, $\gamma = 0.5$, respectively. (b) The S_L as a function of $\log_2 L$. The solid, dashed, and dotted lines correspond to the points in the Ising transition line at $h = 1.0$, $\gamma = 0.5$ and in region III at $\gamma = 0.2$, $h = 0.5$, $h = \sqrt{4D^2 - 2\gamma^2 + 1} = 1.039$ for $D = 0.2$, respectively.

Therefore, under the effects of the DM interaction, the critical behaviors of the XY chain for $0 < \gamma < 2D$ and $0 < h \leq \sqrt{4D^2 - \gamma^2 + 1}$ are similar to that of the XY chain in a transverse field without the DM interaction for $\gamma = 0$ and $0 < h \leq 1$. And the properties of the chiral phase are distinctively different from the FM and PM phases, where S_L is always a nonzero constant.

5. Conclusion

In summary, we have studied the effects of the DM interaction on the ground-state properties of the XY chain in a transverse field. By the analytical and numerical results we find that (i) a gapless chiral phase is induced by the DM interaction for $\gamma < 2D$; (ii) from the chiral phase to the FM (or PM) phase , the QPTs are like those in the anisotropy transition; (iii) the von Neumann entropy S_L in the chiral phase is proportional to $\log_2 L$ with the coefficient $A \approx 1/3$, which is the same as that of the XY chain in a transverse field without the DM interaction for $\gamma = 0$ and $0 < h \leq 1$. Moreover, the above ground-state properties mainly attribute to the special excitation spectra which are not symmetrical in the momentum space and are not always positive.

Acknowledgment

We thank Li Wen-Juan and Xiong Ye for useful discussions.

References

[1] Dzyaloshinshy I 1958 *J. Phys. Chem. Solids* **4** 241
[2] Moriya T 1960 *Phy. Rev.* **120** 91
[3] Seki S, Yamasaki Y, Soda M, Matsuura M, Hirota K and Tokura Y 2008 *Phys. Rev. Lett.* **100** 127201
[4] Li Q C, Dong S and Liu J M 2008 *Phys. Rev. B* **77** 054442
[5] Sergienko I A and Dagotto E 2006 *Phys. Rev. B* **73** 094434
[6] Oshikawa M and Affleck I 1997 *Phys. Rev. Lett.* **79** 2883
[7] Zhao J Z, Wang X Q, Xiang T, Su Z B and Yu L 2003 *Phys. Rev. Lett.* **90** 207204
[8] Kohgi M, Iwasa K, Mignot J M, Fak B, Gegenwart P, Lang M, Ochiai A, Aoki H and Suzuki T 2001 *Phys. Rev. Lett.* **86** 2439
[9] Veillette M Y, Chalker J T and Coldea R 2005 *Phys. Rev. B* **71** 214426
[10] Tsukada I, Takeya J T, Masuda T and Uchinokura K 2001 *Phys. Rev. Lett.* **87** 127203
[11] Messio L, Cepas O and Lhuillier C 2010 *Phys. Rev. B* **81** 064428
[12] Huh Y, Fritz L and Sachdev S 2010 *Phys. Rev. B* **81** 144432
[13] Wernsdorfer W, Stamatatos T C and Christou G 2008 *Phys. Rev. Lett.* **101** 237204
[14] Zakeri K, Zhang Y, Prokop J, Chuang T H, Sakr N, Tang W X and Kirschner J 2010 *Phys. Rev. Lett.* **104** 137203
[15] Jafari R, Kargarian M, Langari A and Siahatgar M 2008 *Phys. Rev. B* **78** 214414
[16] Jafari R and Langari A 2008 arXiv: 0812.1862v1 [cond-mat.str-el]
[17] Derzhko O, Verkholyak T, Krokhmalshii T and Büttner H 2006 *Phys. Rev. B* **73** 214407
[18] Verkholyak T, Derzhko O, Krokhmalskii T and Stolze J 2007 *Phys. Rev. B* **76** 144418
[19] Kádár Z and Zimborás Z 2010 *Phys. Rev. A* **82** 032334
[20] Kargarian M, Jafari R and Langari A 2009 *Phys. Rev. A* **79** 042319
[21] Li Y F and Kong X M 2013 *Chin. Phys. B* **22** 037502
[22] Chen T, Huang Y X, Shan C J, Li J X, Liu J B and Liu T K 2010 *Chin. Phys. B* **19** 050302
[23] Wang L C, Yan J Y and Yi X X 2010 *Chin. Phys. B* **19** 040512
[24] Liu B Q, Shao B, Li J, Zou J and Wu L A 2011 *Phys. Rev. A* **83** 052112
[25] Siskens T J, Capel H W and Gaemers K J F 1975 *Physica* **79A** 259
[26] Amico L, Fazio R, Osterloh A and Vedral V 2008 *Rev. Mod. Phys.* **80** 517
[27] Wootters W 1998 *Phys. Rev. Lett.* **80** 2245
[28] Bennett C, Bernstein H, Popescu S and Schumacher B 1996 *Phys. Rev. A* **53** 2046
[29] Osterloh A, Amico L, Falci G and Fazio R 2002 *Nature* **416** 608
[30] Pfeuty P 1970 *Ann. Phys.* **57** 79
[31] Zhong M and Tong P Q 2010 *J. Phys. A: Math. Theor.* **43** 505302
[32] Vidal G, Latorre J I, Rico E and Kitaev A 2003 *Phys. Rev. Lett.* **90** 227902
[33] Holzhey C, Larsen F and Wilczek F 1994 *Nucl. Phys. B* **424** 443
[34] Lieb E, Schultz T and Mattis D 1961 *Ann. Phys.* **16** 407
[35] Tong P Q and Liu X X 2006 *Phys. Rev. Lett.* **97** 017201
[36] Kawamura H 1988 *Phys. Rev. B* **38** 4916
[37] Stolze J, Viswanath V S and Müller G 1992 *Z. Phys. B* **89** 45
[38] de Oliveira T R, Miranda E, Rigolin G and de Oliveira M C 2008 *Phys. Rev. A* **77** 032325
[39] Barouch E and McCoy B 1971 *Phys. Rev. A* **3** 786
[40] McCoy B, Barouch E and Abraham D 1971 *Phys. Rev. A* **4** 2331
[41] Müller G and Shrock R 1985 *Phys. Rev. B* **32** 5845
[42] Keating J P and Mezzadri F 2004 *Commun. Math. Phys.* **252** 543